

## Experimental Investigation on Electrical, Thermal and Wear Behaviour of AL6061-Ag Composite

Rumaisa Farooq<sup>1</sup>, Er. Neeraj Kumar<sup>2</sup>

<sup>1</sup>PG SCHOLAR, DEPARTMENT OF MECHANICAL ENGINEERING, R N COLLEGE OF ENGINEERING & TECHNOLOGY, MADLAUDA, PANIPAT

<sup>2</sup>ASSISTANT PROFESSOR, DEPARTMENT OF MECHANICAL ENGINEERING, R N COLLEGE OF ENGINEERING & TECHNOLOGY, MADLAUDA, PANIPAT

Email id :- [rumisafarooq96@gmail.com](mailto:rumisafarooq96@gmail.com)

### Abstract

*The research work focuses on the experimental investigation of the mechanical, electrical and thermal behavior of cast aluminum 6061 with different content of silver, 3, 6, 9 & 12% by weight basis. Al6061 composite were produced by means of stir casting. By increasing the percentage of Ag constituents in Al6061 matrix, the electrical conductivity increases because of superior electrical properties produced by Ag constituents. Thermal gravimetric analysis (TGA) was performed using Jupiter thermal analyzer to quantify the degradation features of Al6061-Ag composite in nitrogen atmosphere having a flow rate of 20mL/min to establish an inert atmosphere to avoid any oxidative decomposition. Dry sliding wear of cast samples were determined by using Pin on disc testing apparatus. Pin specimens of ASTM G99 were machined from cast samples. The pin specimens were then slid beside an EN 31 steel hardened to 60HRC. The pins were cautiously cleaned with acetone and weighed using a sensitive electronic balance to determine the weight loss. Specific wear rate was determined in terms of weight loss data. The specific wear rate was mainly influenced by the input parameter weight % of silver, load and sliding distance. The coefficient of friction was calculated from the observed frictional force and applied load. Worn surface and debris particle studies were effectively carried out to know the wear mechanism. Energy Dispersive Spectroscopy (EDS) was used to detect the elements present in the Al6061-Ag composites.*

**Keywords:-** Experimental investigation, Al6061, Ag, composite, EDS.,

### INTRODUCTION

A composite material is made by combining two or more materials – often ones that have very different properties. The two materials work together to give the composite unique properties. However, within the composite one can easily tell the different materials apart as they do not dissolve or blend into each other. For example, concrete is a composite because it is a mixture of Portland cement and aggregate. Fiberglass sheet is a composite since it is made of glass fibers imbedded in a polymer.

Composite materials can take many forms, but they can be separated into three categories based on the strengthening mechanism. These categories are dispersion strengthened, particle reinforced and fiber reinforced. Dispersion - strengthened composites have a fine distribution of secondary particles in the matrix of the material. These particles impede the mechanisms that allow a material to deform.

If the composite is designed and fabricated correctly, it combines the strength of the reinforcement with the toughness of the matrix to achieve a combination of desirable properties not available in any single conventional material. Some composites also offer the advantage of being tailorable so that properties such as strength and stiffness can easily be changed by changing the amount or orientation of the reinforcement material. Such composites are often more expensive than conventional materials. The advantages of using composite materials include :

- ❖ Resistance – To a wide range of chemical agents including acid rain and salt spray, conditions under which metal parts would suffer. This results in much reduced maintenance and repair costs.

- ❖ Resilience – The ability to deform and spring back to their original shape without major damage. Shape memory and impact tolerance are two of the biggest advantages of composites, particularly within the transport industry.
- ❖ Low weight – With substantial savings in weight over similar metal parts (25% the weight of steel, 30% lighter than aluminium), cost savings are noticeable with installation, handling and particularly fuel consumption, when in service.
- ❖ Adhesive and coating compatibility – Since composites and adhesives/coatings share a similar polymeric make-up, they are widely compatible with one another.
- ❖ Thermal properties – Composite structures act as very good insulators, whilst retaining their shape, without becoming brittle in cold temperatures.
- ❖ Strength – Comparable to aluminium and steel, strength characteristics of many materials can be reproduced through research and development with reinforcements, e.g. glass.
- ❖ Innovative designs - which were previously impractical can be achieved with composites with no loss in performance or strength.
- ❖ Safety – Fibre reinforced composites are low in electrical conductivity and are efficient fire retardants, which make them a good choice for covering electrical parts.

### *A. Melting and pouring*

#### **a) Cleaning of Materials**

A successful effort in removing the oxides that stick on the crucible's wall as well as bottom in the prior melting could only be achieved if the oxides are dissolved. This is attainable if the filling of the crucibles is made, while keeping it for five hours. Subsequently, it is cleaned using the MS wire brush. The metallic wire brush is used to clean every steel tool employed in the melting process as well as the purpose of pouring.

The metal ingots thereafter cleaned with the employment of acetone. Every tool as well as metal ingots undergo preheating prior to usage. The mould, after being well cleaned will have the graphite coating applied to it and will then be preheated to a temperature of 250°C, using the heating oven for the period of one hour prior to casting.

#### **b) Melting**

The melting arrangement for Al6061-Ag composites is presented in Figure 1. Resistance table top furnace has been used for melting. The preheated flux is sprinkled in the bottom and side of the cleaned crucible and kept inside the furnace. After the crucible reaches the red hot condition, the preheated Al6061 ingots are charged into the crucible. Initially, part of the total ingots are charged. After melting of the charged ingots is completed, the remaining ingots are immersed into the molten Al6061. This kind of charging practice of metal ingots avoids the excessive oxidation during melting. Crucible is covered with furnace cover to minimize the air contact with the molten metal. Flux is sprinkled over the metal throughout the melting.

The alloy temperature is increased to about 710°C. With a view to get a uniform temperature condition, the melt is positioned at the preset temperature for 30min. An impeller made from alumina coated stainless steel and driven by a variable speed DC motor is used to stirred the molten metal mechanically at a speed of 550rpm. The wettability of Ag particles in Al6061 has been enhanced by adding 1wt.% of Mg into the Al6061 melt. At a temperature of 760°C for a time period of twenty minutes the heated silver particles are added into the molten alloy. Before addition of Ag particles, the top layer of oxides is completely removed, and a fresh layer of flux is applied. The required amounts of heated silver particles are weighed and wrapped in aluminum foil and are slowly immersed into the melt. After additions, the melt is gently stirred for dissolution of the added elements. Again, the top oxide layer is removed, and a fresh layer of flux is applied. The melt is held for 20 min to ensure complete dissolution of elements into the melt (Saravanan et al. 2016).

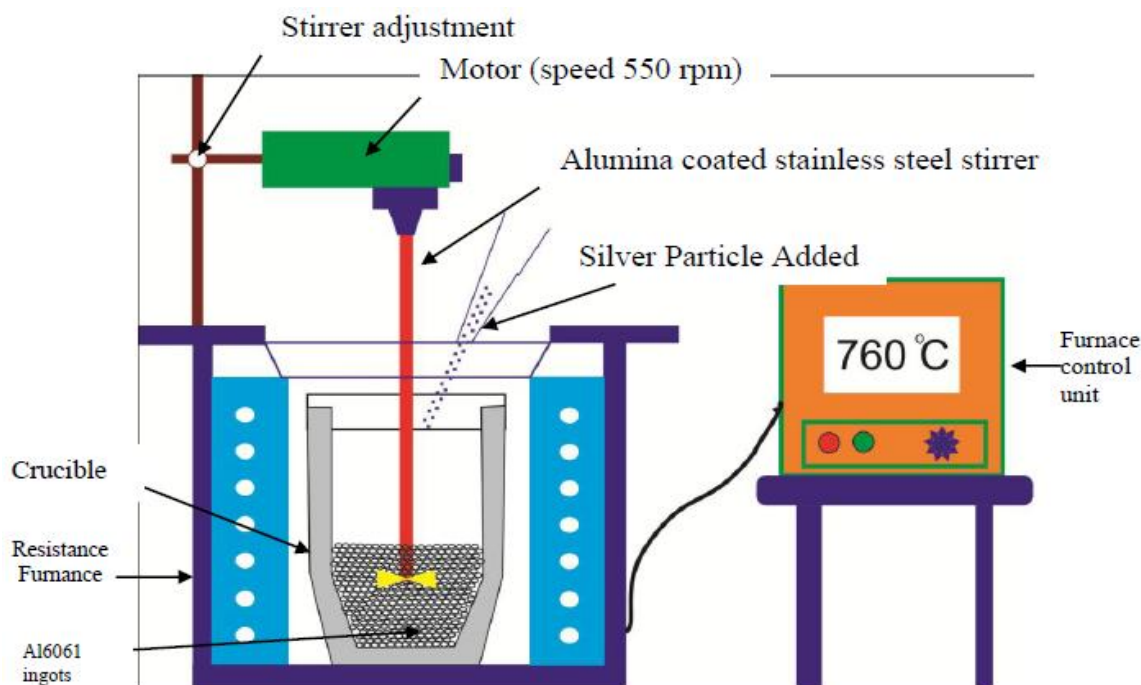


Figure 1:- Schematic illustration of the stir casting setup

### c) Pouring and Casting

After the melting and stirring process are over, the molten metal is poured into the preheated moulds. During pouring, much care is taken to avoid the breakage of top flux protective layer. The pouring is carried out gently without any jerk in the melt since excessive jerk disturbs the settled oxide inclusions in the bottom. The flux layer near the lip of the crucible is pulled back gently by using a skimmer for smooth flow of molten metal. Sulfur powder dusting is carried out to remove the oxygen around the melt jet. Three fourths of the melt in the crucible is poured into the preheated mould. The remaining metal is poured separately as a scrap. After that, the solidified casting is detached from the mold. Using the above - described casting procedure, different combinations (3, 6, 9, 12 wt.%) are prepared for the present study.

### B. Chemical analysis

To find out the actual elemental compositions in the composites prepared, chemical analysis have been carried out. Chemical analysis of most of the elements in the prepared composite is carried out using conventional wet analysis technique based on the procedures given in the ASTM standards (Table 1). However, some of the alloy compositions are found out using inductively coupled plasma spectrometer (ICP Plasma scan, model: LABTAM8410). The major elements like Si, Mg, Cu, etc. in all the prepared castings are carried out. The analyzed alloy compositions are presented in Table 1

Table 1: Results of chemical analysis of the cast composites

Specimen details	Analysed Composition, wt. %					
	Si	Fe	Mg	Cu	Zn	Ag
Al6061	0.75	0.41	0.92	0.26	0.07	-
Al6061-3%Ag	0.74	0.44	0.87	0.24	0.06	2.87
Al6061-6%Ag	0.72	0.43	0.86	0.25	0.05	5.94
Al6061-9%Ag	0.65	0.42	0.84	0.23	0.05	8.87
Al6061-12%Ag	0.67	0.43	0.85	0.22	0.04	11.92

## **MICROSTRUCTURAL OBSERVATION**

### *A. Sample Preparation*

To avoid the variation in microstructure and properties along the thickness of the casting and maintain the uniformity in microstructure, all the samples are taken from the center portion of the castings. Cylindrical pieces of 15 mm diameter and 10mm height are machined out from the cast specimen. The surface of the sample, which is nearer to the wall surface of the castings is selected for further characterization (microstructure and hardness measurement).

#### **a) Polishing**

Initially, the samples were polished using different grades of emery papers of progressively fine grades of 80, 220, 400 and 600 grits. During paper polishing, water is used as a cleaning agent. Once the paper polishing was completed the samples are polished in a rotating disc of selvyte cloth charged with a diamond paste of 6, 3 and 0.25  $\mu\text{m}$  particle size in order. Filtered kerosene is used as lubricant during cloth polishing. Samples are gently pressed against the rotation wheel. Since magnesium is a soft material, much care is taken during polishing to avoid sketches and excessive surface contamination. Cleaning the samples with distilled water is found inefficient to take out surface contaminants of the polished samples. So, after the final polishing is over, the surface of the samples is cleaned using ultrasonic cleaner in ethanol.

#### **b) Chemical Etching**

Different kinds of etchants are tried to get a clear microstructure. After various trials, picric acid based etchant is found to be an efficient one, which clearly reveals the micro constituents of aluminium. The traditional mechanical polishing and etching in Keller and Weck reagents (upto10s) are used to prepare the specimens for the micro structural studies. Much care is taken during etching to avoid over etching, otherwise, it would spoil the surface of the samples.

#### **c) Optical Microscope**

Microstructural specimens (after polishing and etching) are observed under a Leitz-Metalloplan optical microscope. Photographs are taken at different locations with various magnifications.

### *B. Density and porosity measurement*

The theoretical densities of Al6061-Ag composites are calculated using rule of mixture. Using the Archimedes principle the actual density of the composite specimens is carried out. The specimens are weighed through an electronic balance with an accuracy of 0.001mg (Make: Sartorius, Model: BS 224S). The actual density is calculated from Equation 1).

$$\text{Density } (\rho) = \text{mass } (m) / \text{volume } (v) \quad (1)$$

$$m = W_a$$

$$v = W_a - W_w$$

where,

$$\rho = \text{Actual Density, g/cm}^3$$

$W_a$  = Composite specimens are weighed in air, g

$W_w$  = Composite specimen fully immersed in water and weighed, g

The relative density of the Al6061-Ag composite samples is determined from the ratio of the actual density to the theoretical density. The residual porosities of Al6061- Ag composites are 1.8 % - 3.9 %.

**Table 2: Density values of cast Al6061-Ag composites**

<b>Composition Details</b>	<b>Theoretical density, kg/m<sup>3</sup></b>	<b>Actual density, kg/m<sup>3</sup></b>	<b>Relative density, kg/m<sup>3</sup></b>
Al6061	2730	2680	98.16
Al6061-3% Ag	2962	2897	97.78
Al6061-6% Ag	3195	3105	97.16
Al6061-9% Ag	3428	3322	96.9
Al6061-12% Ag	3661	3518	96.1

### C. Hardness

The employed hardness equipment, by make, is the INTENDEC employed for Brinnell hardness appraisal of cast specimens. The specimen's faces were made level for the two sides. Planning of a side of the specimen in which the appraisal of hardness is to be made. For the polishing exercise the 600fine emery paper was employed while the purpose was to do away with the oxide as well as other scales in order to clearly see through the edges of the marks ( i.e. indentation).The indentation was achieved with the aid of a 10 mm ball. A load of 500g was the fixed load while working for 30 sec, referred to as the dwell time. A total of four indentations were recorded while the real value use was the average of the four.

### D. Electrical resistivity

The popular four-point probe tester was used to find out the electrical resistivity in this experiment. According to the ASTM B193 standard the sample was prepared. Generally, electrical resistivity measures how much a given material resists the flow of electrons. Copper is the matrix metal selected for this study, it has good electrical conductivity when compared with those of any other metals (Selvakumar et al. 2014).The electrical resistivity test was carried out in a dynamic nitrogen atmosphere with a constant current of(I = 0.5 A) and different temperature. The size of the test specimens was 12mmdiameter and25 mm length. A fine-grade emery sheet was used to polished the composite specimens to get better contact before testing. A thermocouple was used to change the temperature when the test was conducted and DC current was used to obtain measurements of voltage (V). Electrical resistivity calculated by the given relationships,

$$\text{Electrical Resistivity, } \rho = \frac{\text{Voltage (V)}}{\text{Current (I)}} \times \frac{\text{Cross Sectional Area (A)}}{\text{Length of Specimen (L)}} \quad (2)$$

where, 'V' is Measurement of the voltage, 'I' is Constant current, (I = 0.5 Amp) and 'A' and 'L' are the cross-sectional area and length of the test specimens respectively. The electrical conductivity is the reciprocal of resistivity. Conductivity measures in the Siemens/meter could be translated to percentage IACS through the multiplication of the conductivity measures by 1.7241 x10<sup>-6</sup>.

### E. Thermal analysis

An investigation on the thermal characteristics of pure Al6061as well as Al6061-Ag composite was conducted through testing which included the DSC as well as DGA, representing the Differential ThermalGravimetry/Thermal Gravimetric Analyzer, correspondingly. As per the ASTM:E473-11a standard thermal analysis was carried out.

The characteristics due to the crystallization, ignition as well as melting of the composites can was examined through the employment of the TGA as well as DSC, to understand the characteristics of the thermal decay for the pure Al6061 and Al6061-Ag composite. The integral of thermal gravimetric analyzer and derivative differential scanning calorimetry curves furnish the deals concerning the stability of the composites (i.e.thermal) as well as the quantity of material degradation. The report showed that an increase was experienced up to 950°C from the normal atmosphere situation through 20°C increase for every interval.

### F. Wear test

As per the ASTM G99-05 standard Al6061-Ag composite specimens prepared for wear tests using pin-on-disc wear testing machine, and the test was carried out in air at room temperature.The disc was made out of EN 31 steel which was hardened to 60HRC. The performs had cylindrical shape having the size of the test specimens was 10mm diameter, and 30mm height.The loading of the composite's pin against the disc was made in the mode referred to as the dead-weight loading scheme. The acetone compound was employed in cleaning the samples as well as the disc. This was done to ascertain the conduct of the wear tests in the circumstances on normal dry sliding experiments (Dwivedi et al. 2006).

The specific wear rate was measured by volume loss method by using the formula is shown in equation(3.3).While the wear testing was done, the frictional force was measured by the wear testing machine, and the frictional force also was changed into coefficient of friction by using Equation (3.4) (Vettivel et al. 2013). The experiment was conducted with applied loads between 10 and 30 N with an increment of 5 N. The sliding speed and track diameter were set at 3.14 m/s and 100mmrespectivelyfor all the specimens. During the wear test an EN 31 steel disc with 60 HRC was made use of the sliding disc of the pin. Figure 2 shows a diagram of the pin-on-disc apparatus.

$$\text{Specific wear rate} = \text{Volume loss}/(\text{Load} \times \text{Sliding distance})(\text{mm}^3 / \text{N}\cdot\text{m}) \quad (3)$$

$$\text{Coefficient of friction} = \text{Frictional force} / \text{Applied load} \quad (4)$$

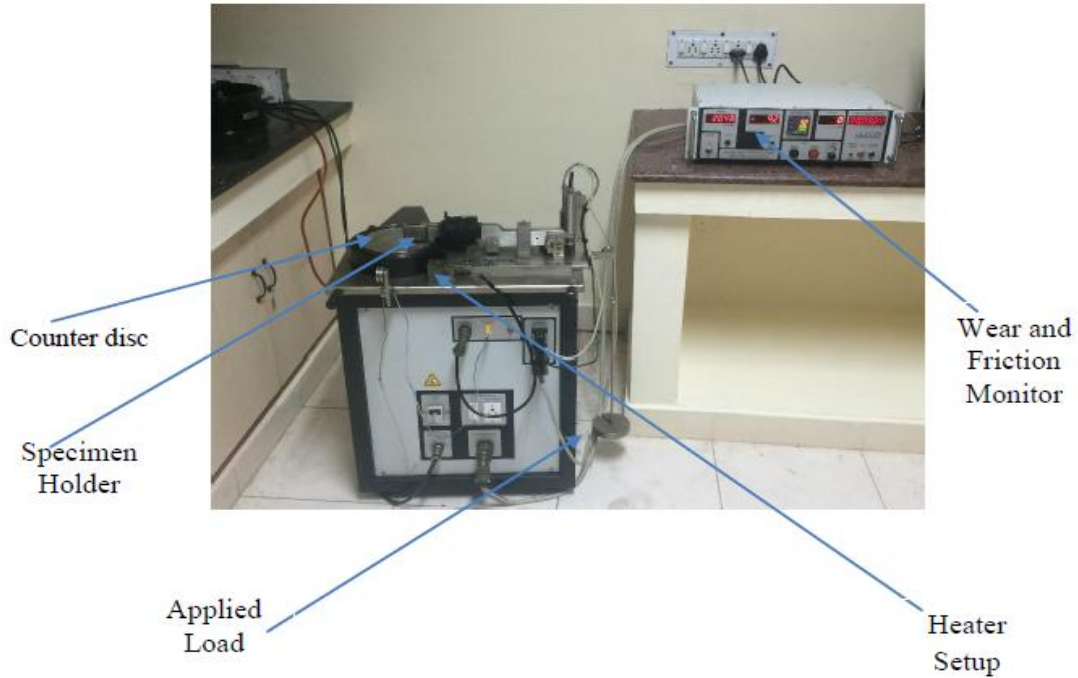
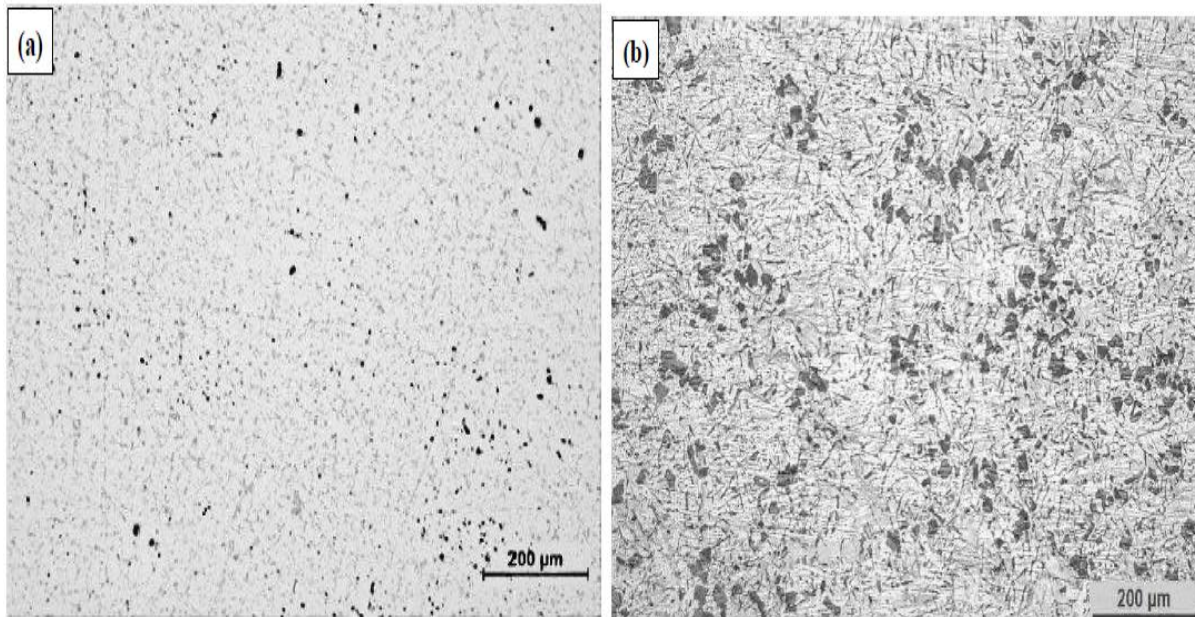


Figure 2:- Pin-on-disc wear testing apparatus

### MICROSTRUCTURAL CHARACTERIZATION

The distribution of Ag occupies a significant position in the microstructures and total accomplishment. The optical micrographs of the Al6061 and the Al6061-Ag composite after polished mechanically are shown in Figure 3. The distribution of micron Ag is nearly uniform in the matrix, and it is uniformly distributed along the surface.



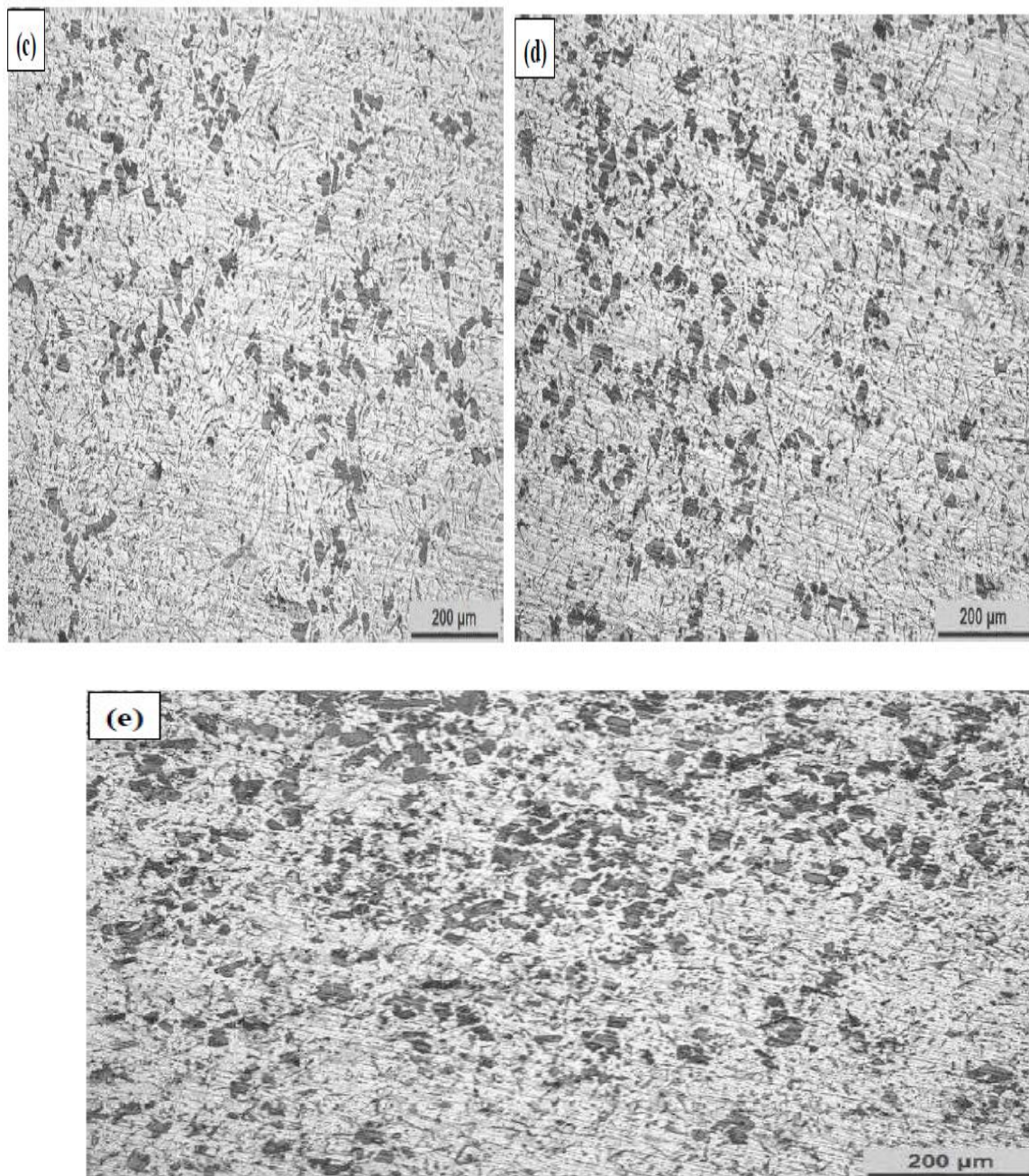


Figure 3:- Optical micrographs of cast (a) Al6061 (b) Al6061-3wt.% Ag (c) Al6061-6wt.% Ag (d) Al6061-9wt.% Ag and (e) Al6061-12wt.% Ag Composite

## RESULTS AND DISCUSSIONS

### A. Physical and mechanical characterization

Figure 4 shows the changes in the density of cast Al6061 and the Al6061-Ag composites. However, it shows a weak increasing trend with an increasing weight percentage of Ag (Table 3). The Brinnell hardness of the cast specimens with a 10mm ball indenter and 500g load for a dwell time of 30sec is illustrated in figure 5. The composites hardness “grows” with the wt.% of reinforcement. These obtained hardness values for Al6061-Ag composite samples are substantially superior to than those for pure Al6061 alloy (91BHN). A hardness of 98 BHN appears at 9 wt.%. No

obvious difference is observed beyond 9 wt.%. This might be associated with the changes in the microstructure with the accumulation of Ag.

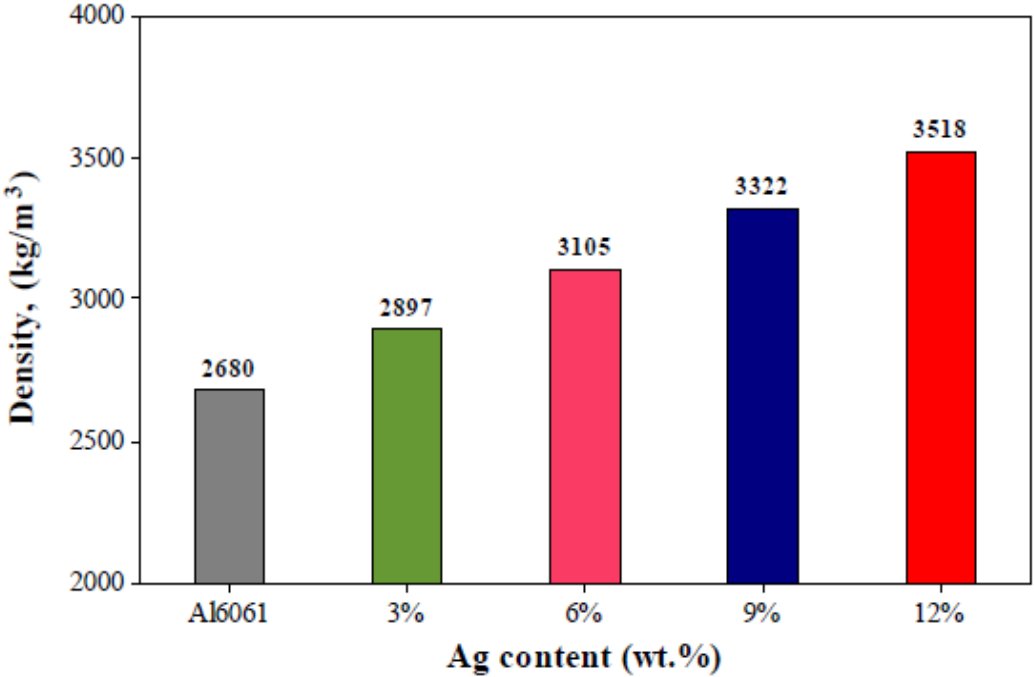


Figure 4:- Density of the Al6061-Ag composite

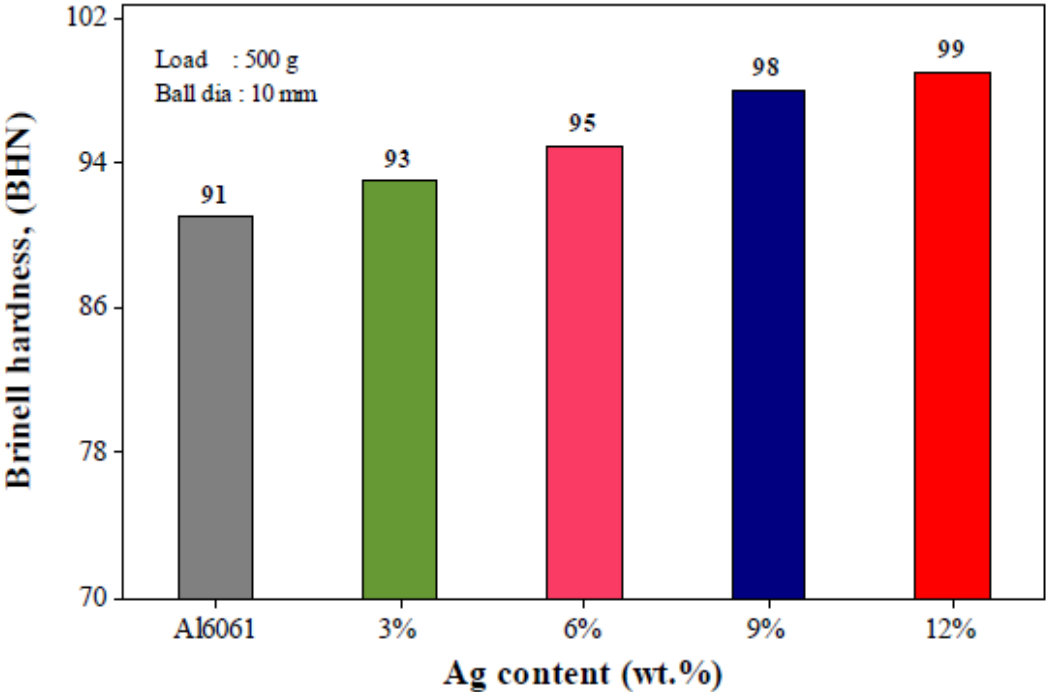


Figure5:- Hardness of the Al6061-Ag composite



*B. Electrical resistivity measurement*

Figure 6 shows the electrical conductivity calculated by equation ( $\rho = V/I \times A/L$ ), of the cast Al6061 and Al6061-Ag composites for different weight fractions. The conductivity linearly increases with increasing weight fraction of Ag. It is the main factor to the conductivity of the composites that the scattering effect is strengthened on the interfacial bonding between the Ag and the Al6061 matrix and the interface between the secondary Ag particle and the Al6061 matrix and the grain boundary decreases the electrical resistance of the composites. Comparing all the samples, it is found that the conductivity of the Al6061-9% Ag composite is higher than that by all the other samples as seen in Figure 6.

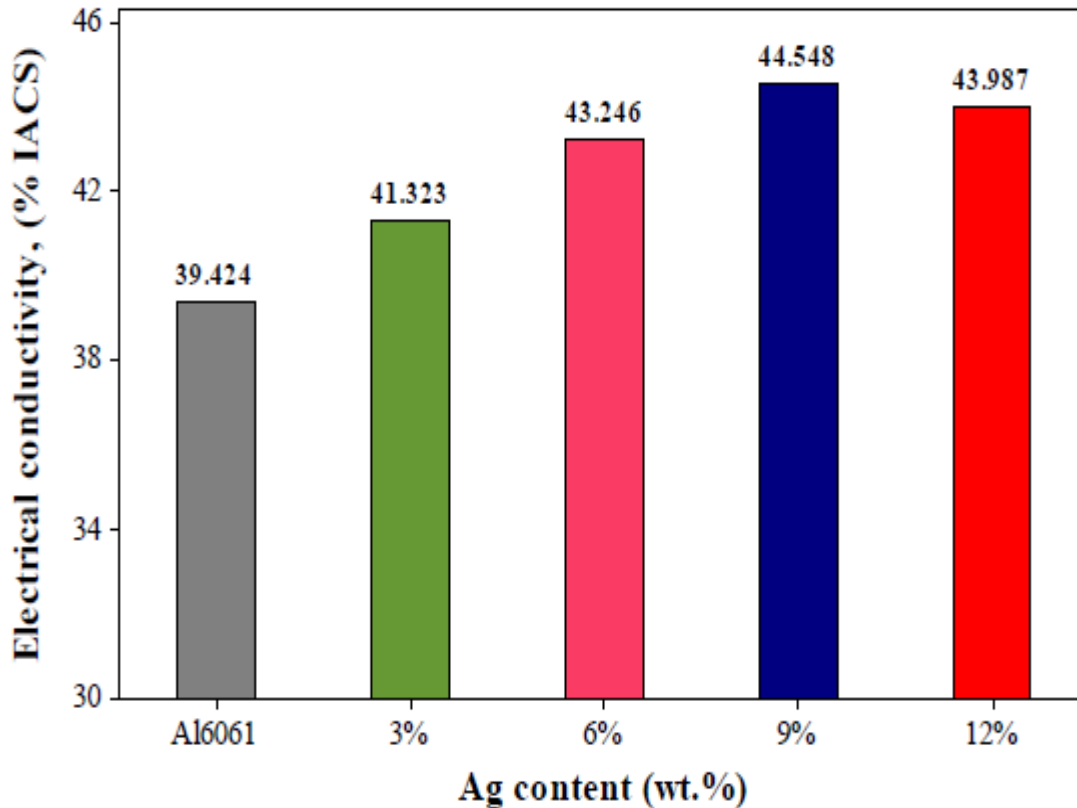


Figure6:- Electrical conductivity of the Al6061-Ag composite

*C. Thermal analysis*

**a) Thermo Gravimetric Analysis**

Figure 7 shows the TG graph of cast Al6061 alloy and Al6061-Ag composite. From Figure7, the maximum weight loss is observed for Al6061 alloy samples with the 4.52 wt. % at 612.56°C, which is due to desorption or drying of samples, thereafter there is a little weight gain up to 660.2°C. Further, with the addition of 12 wt. % of Ag improves the thermal resistance, only 0.258% of weight loss at 669.2°C. For all TG samples, roughly the initial degradation starts around at 135°C. Table 3 shows initial and final degradation temperature of cast Al6061 and Al-Ag composite.

Initially, weight loss is observed for all the composites, when increasing temperature. Initial degradation is more than 500°C temperature for cast Al6061-Ag composite and it is mainly due to desorption, desolation and decomposition of some elements present in the system. Weight loss is from room temperature to 650°C, thereafter little weight is observed up to 750°C in Al6061-Ag composites. This is mainly due to the settlement of solid gas reactions. With the addition of Ag in aluminium matrix increasing the thermal stability of composites, there is 4.69 times better reinforcement than single reinforcement. The maximum weight loss is found in Al6061 composites (4.52%), and minimum weight loss is observed with the inclusion of Ag (0.258%) at 12 % of Ag.

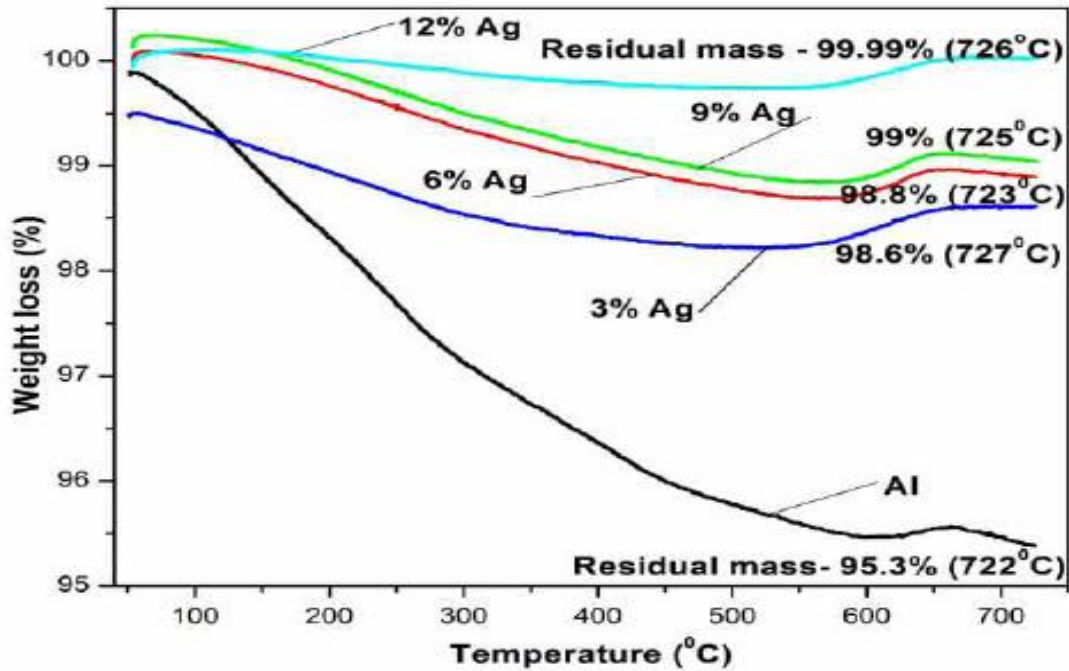


Figure 7:- TGA curve for Al6061-Ag composite

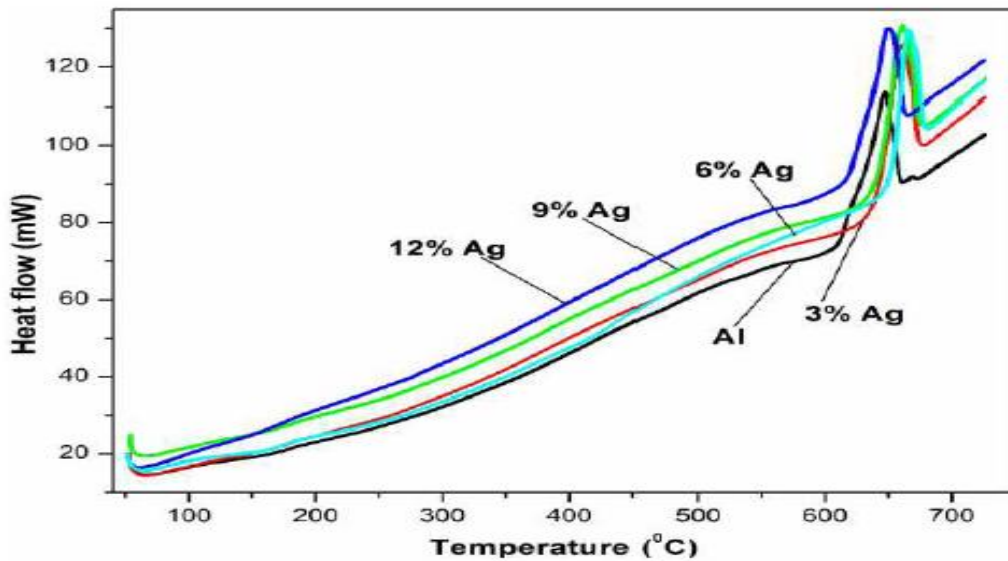


Figure 8:- DSC plot of pure Al6061 & varied Al6061 - Ag composites

Table 3: Degradation and Crystallization temperature of Al6061-Ag composite

Specimen	IDT (°C)	FDT (°C)	% of wt.loss	T <sub>c</sub> (°C)	T <sub>m</sub> (°C)
Al	54.79	589.95	4.52	648.2	659.4
3% of Ag	59.68	582.62	1.76	665.1	676.3
6% of Ag	116.29	573.6	1.32	665.4	681.1
9% of Ag	118.18	570.2	1.17	665.9	685.2
12% of Ag	229.66	476.42	0.258	669.2	685.4

IDT - Initial Degradation Temperature ; FDT - Final Degradation Temperature ;  
T<sub>c</sub> - Crystallisation Temperature ; T<sub>m</sub> - Melting Temperature

#### **b) DSC of Al6061-Ag composite**

Figure 8 shows the DSC plot for Al6061 and Al6061-Ag composites. The degradation and crystallization temperature of Al6061 and Al6061-Ag composites was obtained through the DSC plot, is given in Table 3. The addition of Ag particle in Al6061 matrix shows positive impact on phase temperature, and Al6061 alloy has low crystallization temperature ( $T_c$ ) of 648.2°C. The maximum crystallization temperature is attained at 669.2°C with 12% of Ag. But the increasing trend is shown at 12% of Ag in Al6061 composites. The melting temperature ( $T_m$ ) of cast Al6061 and Al6061-Ag composite, shows gradual improvement in addition of wt.% Ag around 660°C melting of pure aluminum samples, with step up of Ag increasing melting temperature of 685.4°C in 12% of Ag. Thereafter, decreasing trend melting temperature is observed. From the plot, it can be concluded that the addition of Ag increases the melting temperature ( $T_m$ ) and crystallization temperature ( $T_c$ ).

### **D. WEAR BEHAVIOR**

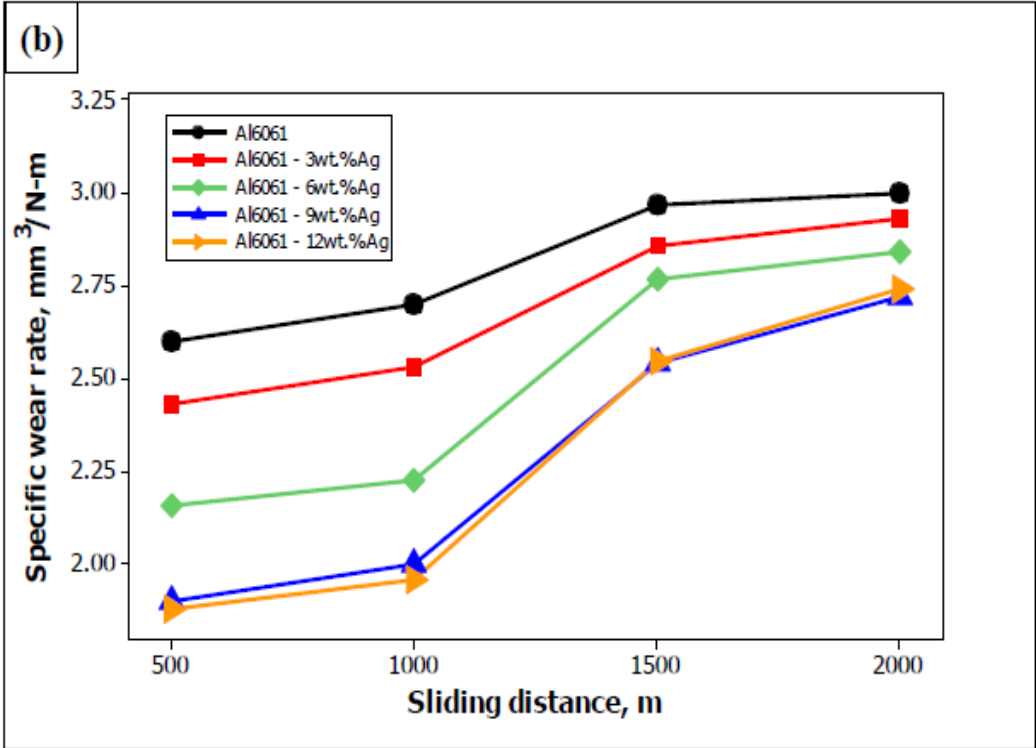
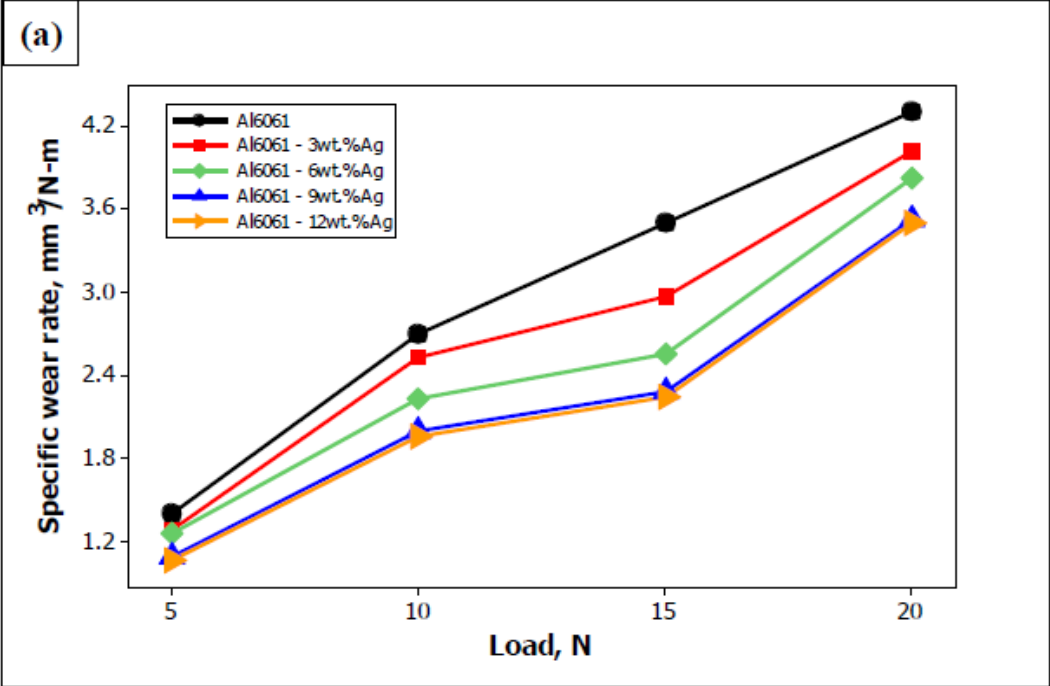
#### **a) Specific Wear Rate**

Pin-on-disc is employed to find out the wear behavior, the parameters of applied load 10N, sliding distance of 1000m and sliding speed of 2m/s. under testing. Figure 9 (a-c) show maximum increases in wear resistance attained after the silver particles are reinforced to Al6061 alloy. The stable decrease in specific wear rate is mainly ascribed to increasing the Ag content up to 9%.

Figure 9(a) shows the difference of specific wear rate with the applied load maintained at a uniform sliding speed of 2m/s and for a fixed sliding distance of 1000m. It is noted that the specific wear rate of the Al6061-Ag composite increases slowly with increase in load up to 15 N after which there is a steep increase in the specific wear rate. The increase in specific wear rate with increased load of all the Al6061-Ag composite specimens studied can be credited to the bigger of plastic deformation quantity as well as delamination wear at superior loads. However, at the highest loading condition, the studied Al6061-9%Ag composite possesses lower wear rates weighed against other Al6061-Ag composite specimens.

Figure 9(b) shows the specific wear rate as depend on the sliding distance. For any given Al6061-Ag composite specimen, the specific wear rate incessantly grows with a growing sliding distance (Ravindran et al.2013). However, it is clearly seen that the wear resistance of the Al6061-Ag composite specimen is significantly better by the accumulation of the reinforcement particles and decreases by increasing Ag weight fraction from 3 to 12 wt.%. For a longer sliding condition, Al6061-9%Ag composite has lower wear rates related to other Al6061-Ag composite samples. This trend may be ascribed to a decrease in the clusters of the silver elements in the Al6061 alloy.

The difference in specific wear rate of the Al6061-Ag composites along with sliding speed is given in Figure 9(c). It is found that an increase in sliding speed leads to decreased specific wear rate of all the samples. The wear test outcome reveal that the specific wear rate of the Al6061-Ag composites is slowly but surely reduced over the range of sliding speeds. However, at all sliding speeds examined, the Al6061-12%Ag composite possesses lower wear rates as weighed against other Al6061-Ag composite specimens. The addition of silver particles, which are released in the course of sliding and then creates a tribolayer at the contact surface causes a reduction in specific wear rate with increase in sliding speeds. With greater than 9% Ag reinforcement addition, the specific wear rate tends to increase at higher load and sliding distance. When all studied load, sliding distance and speeds, were applied comparatively, the Al6061-9%Ag composite has the lowest specific wear rate.



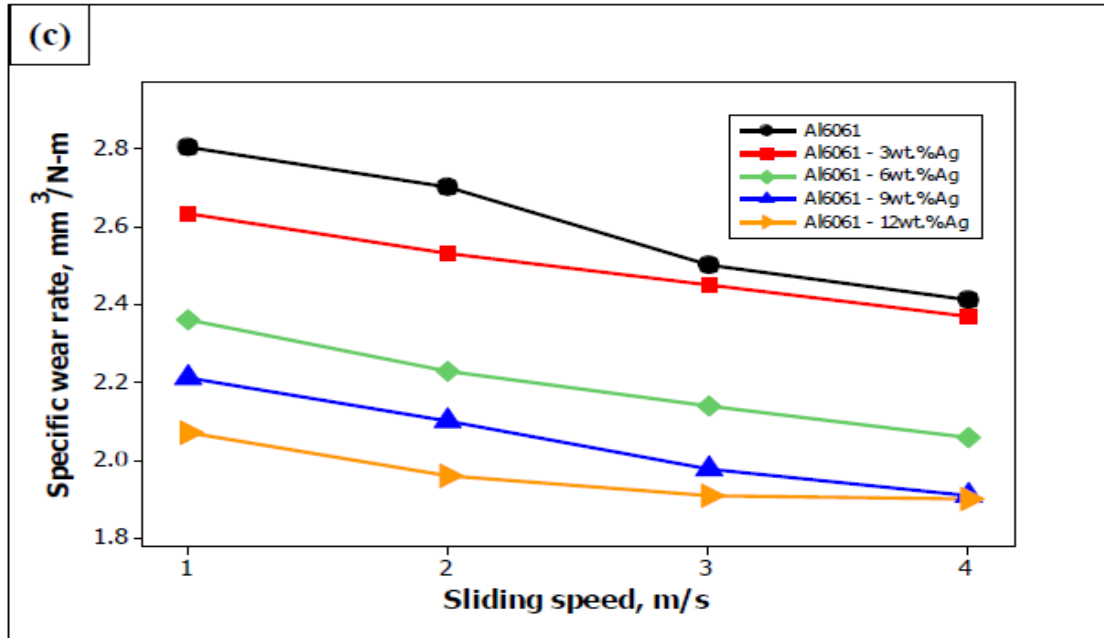


Figure 9:- Specific wear rate of Al6061 and Al6061-Ag composites with  
(a) load (b) sliding distance (c) sliding speed

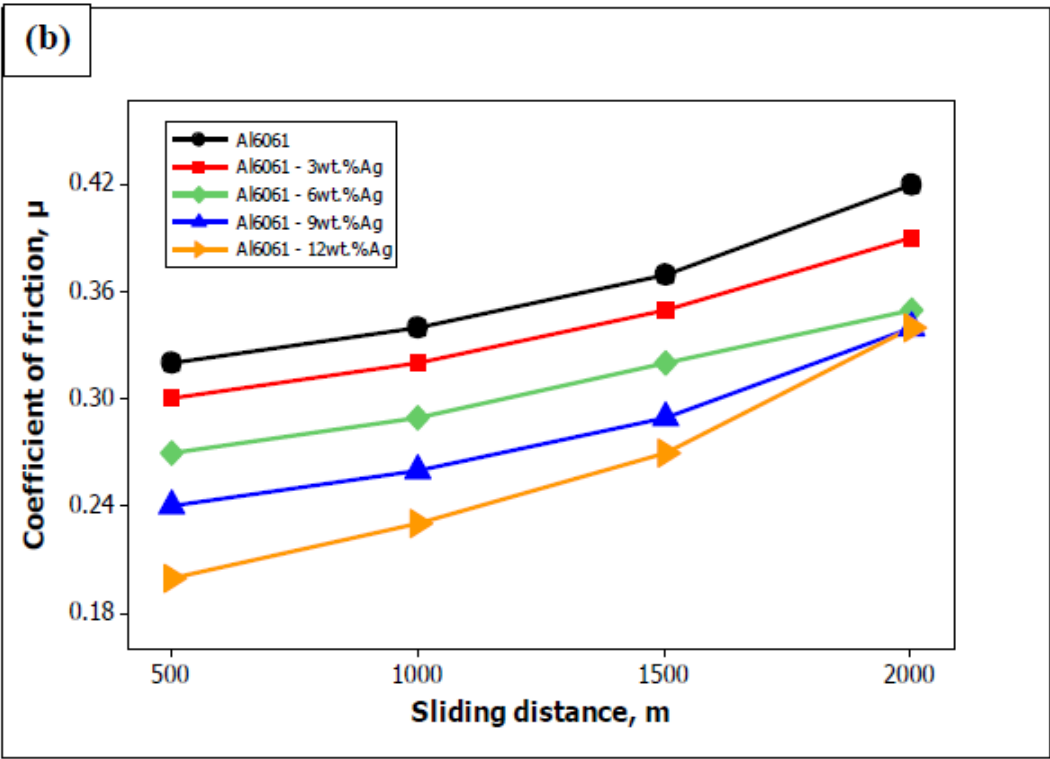
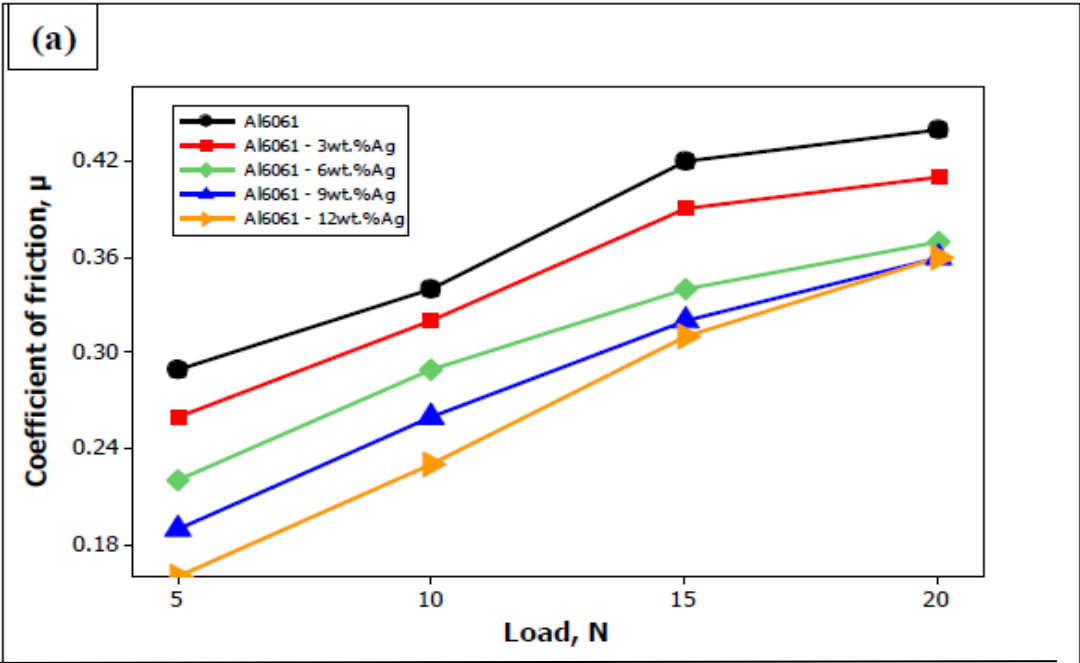
#### b) Coefficient of Friction

The variation of the frictional coefficient (CoF) for the composite specimens as dependent on load, sliding distance and speed are represented in Figures 10(a-c) respectively. Also, Figures 10(a-c) show an influence of percentage weight of Ag in Al6061 matrix on the frictional coefficient of the composites. There is a clear understanding that heightened composition Ag in Al6061 matrix gives in decreased frictional coefficient. There is a well a clear understanding that Al6061-Ag composites display lessened frictional coefficient as weighed against with that of Al6061 matrix. There is no significant improvement in frictional coefficient for Al6061 alloy with more than 9 and 12wt.% Ag content at higher load and longer distances.

Figure 4.8(a) shows variation of applied load and frictional coefficient of Al6061-Ag composites under a uniform sliding distance of 2000 m and speed of 2m/s. The frictional coefficient grows when applied load is grew from 5 to 20 N, as shown in Figure 10(a). It is certainly convincing from this figure that the coefficients of friction of the Al6061-Ag composites are less than those of the Al6061 alloy. A higher frictional coefficient is displayed in Al6061 for all of the load circumstances.

The frictional coefficient of Al6061-Ag composites sliding distance with a constant load of 10N and speed of 2m/s shown in Figure 10(b). An increase in frictional coefficient with increase in sliding distance can be mainly attributed to increased surface temperature. In all the samples, the coefficient of friction values gradually increase up to about 1500m sliding distance, and then increase to reach relatively steady values (0.2–0.4). This trend in the variation of frictional coefficient may be due to the formation of the mechanically mixed layer on the surface. Observed that 9 & 12wt.% Ag composites exhibit the lowest and almost equal coefficient of friction values (Figure 10b). This explanation for this is the occurrence of elevated quantity of oxide compound composition occurring on the worn surface of Al6061-9%Ag composite sample compared to Al6061-9%Ag and Al6061-12%Ag.

The variation of frictional coefficient of Al6061-Ag composite with sliding speed is displayed in Figure 10(c). The decrease of coefficient of friction with grown sliding speed that could be linked to the addition of silver in Al6061 is squeezed out onto the mating surfaces, creating a mechanically mixed layer, and as well the smeared oxide particles form the film in contact surface. A lesser value of the frictional coefficient suggests a less specific wear rate, and the lower frictional coefficient of Al6061-9%Ag composite is the lowest among the other composites tested at higher speeds.



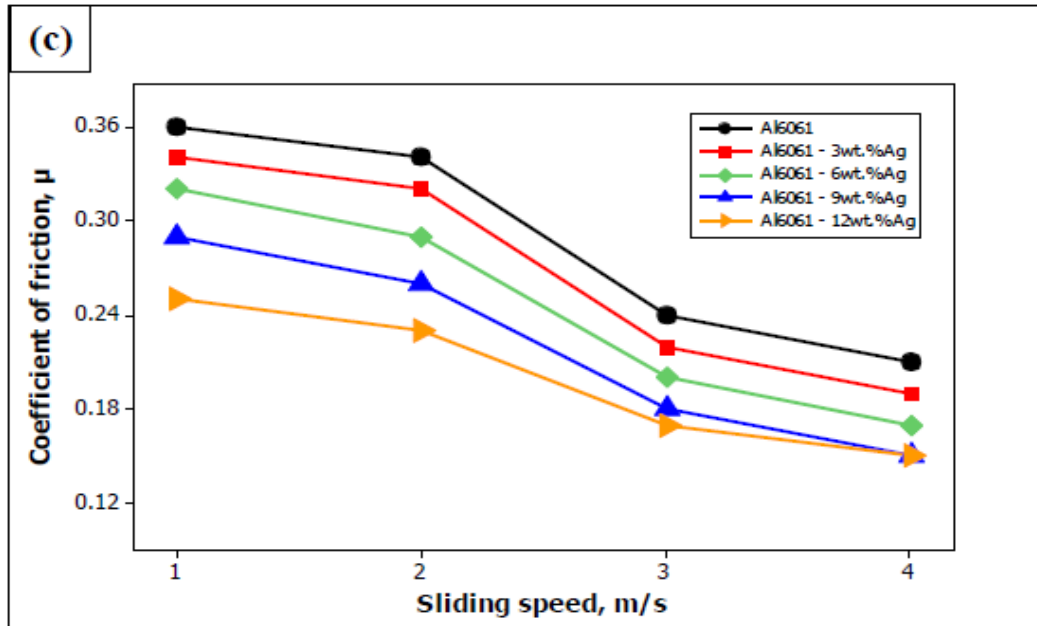


Figure 10:- Variation of coefficient of friction Al6061 and Al6061-Ag composites with (a) load (b) sliding distance (c) sliding speed

### c) Worn Surface Morphology

To determine the wear mechanism on each worn surface, samples have been examined using SEM. Figure 11(a-e) reveals SEM micrographs from the worn surfaces of the 3%, 6%, 9% & 12% samples.

Figure 11(a) represents the SEM micrograph of Al6061 matrix which reveals the brighter layer and reveals the creation of wide wear grooves and some macro cracks (Figure 11a), on the other hand SEM micrograph of bright area shows heavy flow of materials along sliding direction which implies higher level of wear as well as localized adhesion occurring between the surface of the specimen as well as the counter body (Figure 411a). When the disc contacts the composite pin sample, the hard counter steel body disc will compress into the Al6061 specimen. Then, abrasion and adhesion wears occur, which delay the movement between the composite pin and the disc. The built-up of macro cracks is possible because of the dint effect employed by the wear debris from Al6061.

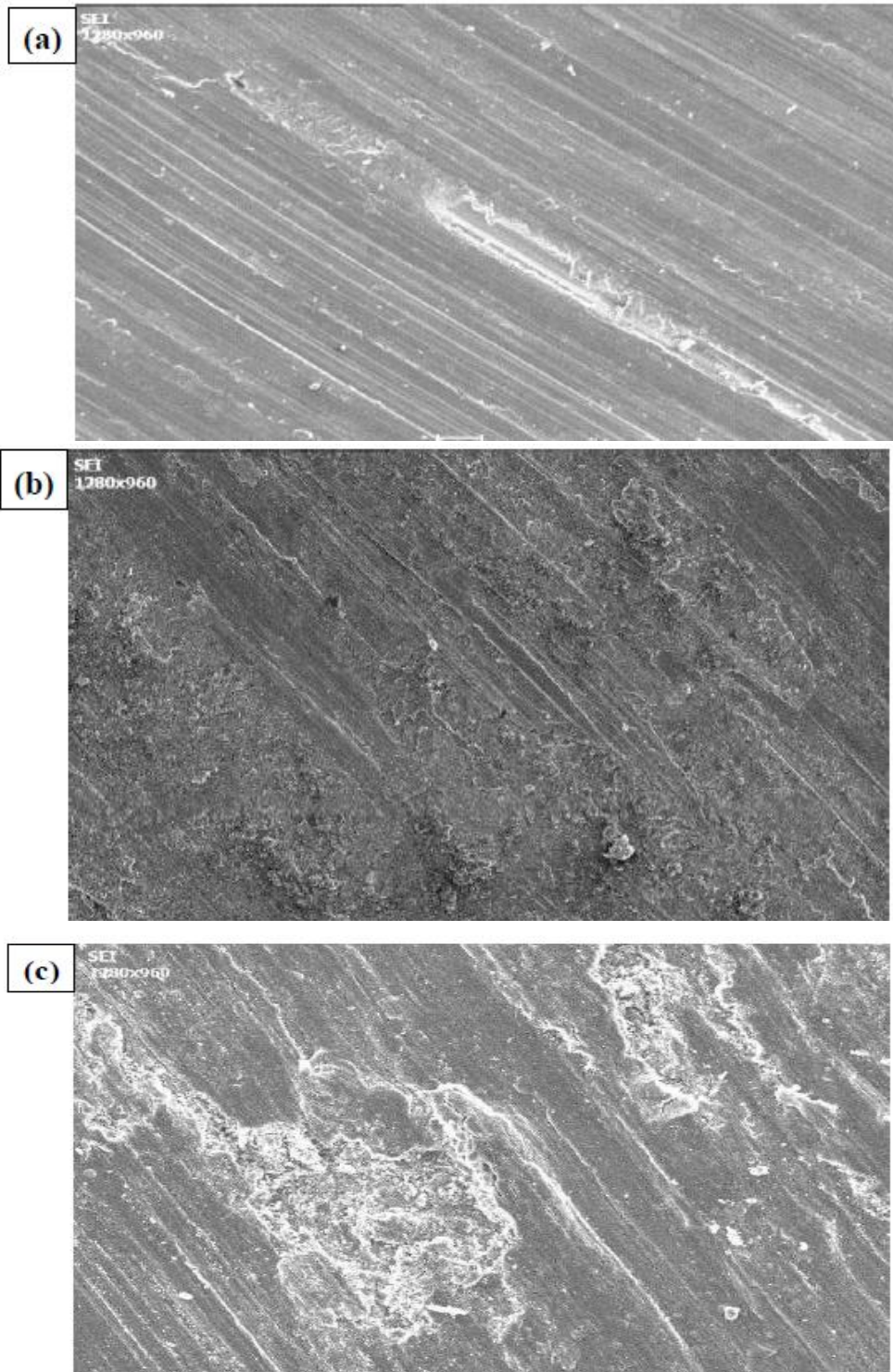
Figure 11(b) is the SEM micrograph of Al6061-3%Ag composite at the post- wear test period. It reveals a transmitting stratum of accumulated wear debris in the course of the wear tracks and could be noticed over the sliding surface. This stratum attains critical thickness prior to detachment, yielding the complete creation of resulting eventually in the generation of wear debris provided by the transfer of excessive delaminating layer. The other cause of lower wear rate in Al6061-3%Ag composite is their increase in hardness compared to Al6061 alloy matrix.

Figure 11(c) reveals the SEM micrograph of Al6061-6%Ag composite after wear test and shows small delamination layers. Addition of 6% Ag reinforcement particles to Al6061 matrix significantly improved the hardness of Al6061-Ag composite and results in a reduction of the extent of delamination deformation of the pin surface. The formed oxide in the course of holding acts as a mechanical mixed tribo layer as protective layer, because of that the specific wear rate of the Al6061-6%Ag composite is considerably lowered.

Figure 11(d) is the SEM micrograph of Al6061-9%Ag composite after wear test and shows that the grooves are created because of plugging through the hard bearing steel ball counter body on the mechanical mixed tribo layers during wear. In comparison to other cases, the tribolayer on the worn surface is thick in nature in the transverse direction and is clearly observed along with deep grooves on the surface.

Figure 11(e) is the SEM micrograph of Al6061-12%Ag composite after wear test and shows that the worn surface reveals agglomeration of fine wear debris particles that are formed at the surface. Such finer debris particles are due to the fracture of oxide layers. While increasing the Ag content from 9% to 12%, merely the minute grooves as well

as debris particle (i.e fine) attain a hard nature and increase specific wear rate. The wear resistance tends to increase with the increasing wt.% of Ag, due to the formation of mechanical mixed layers.





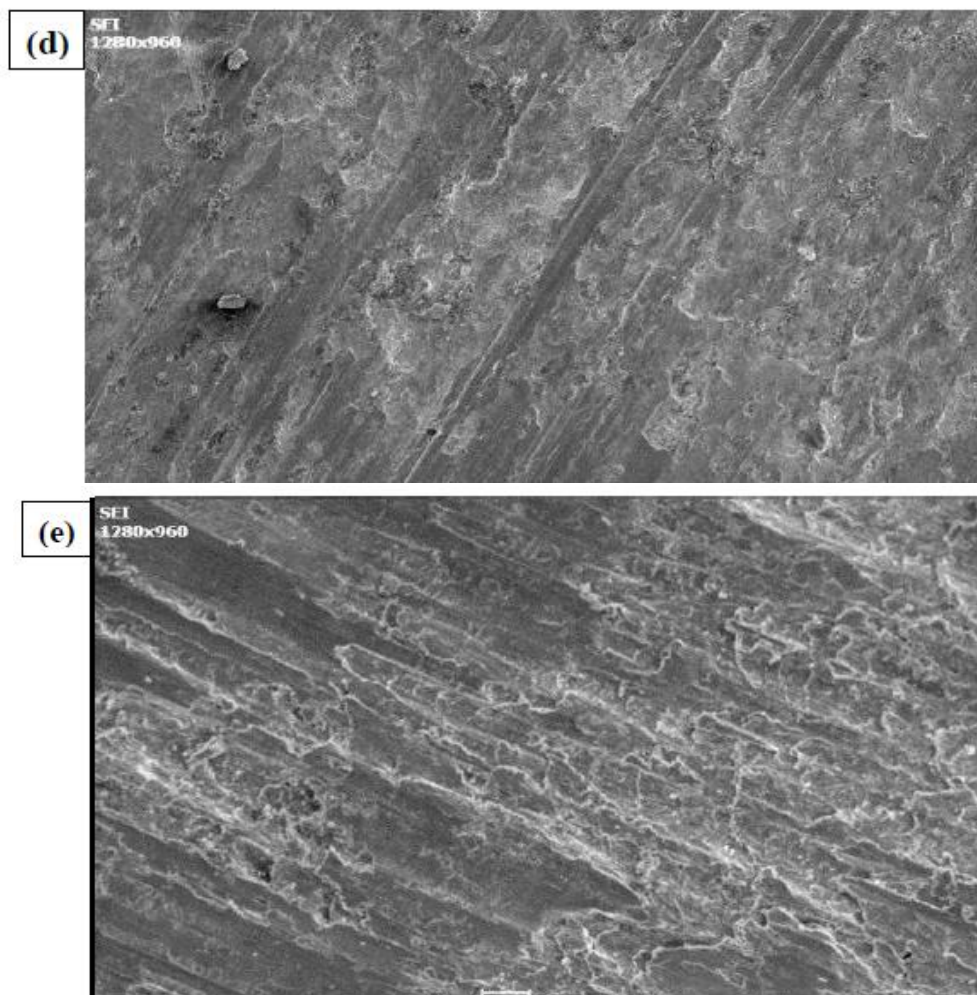
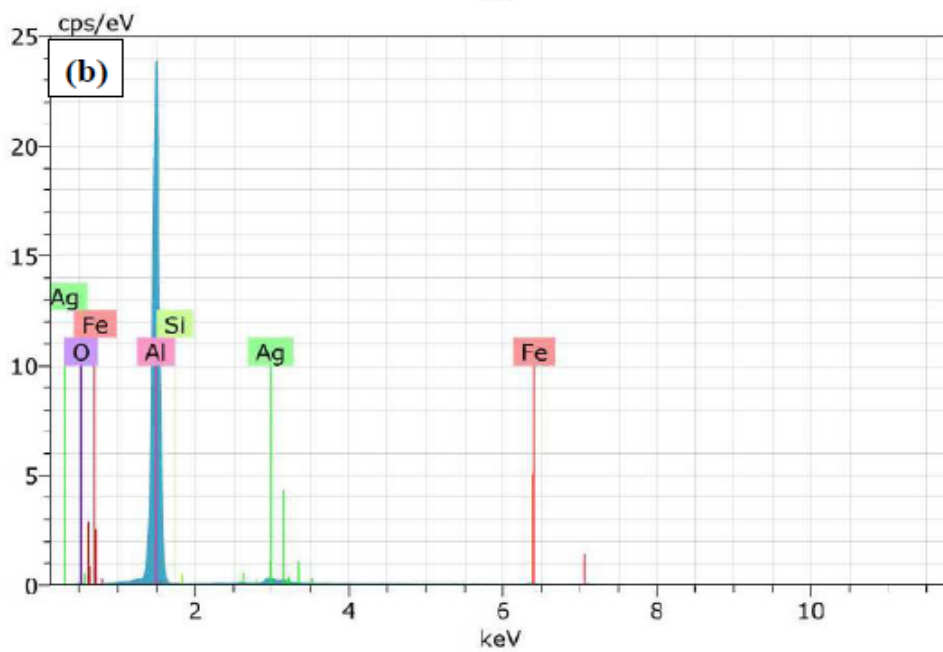
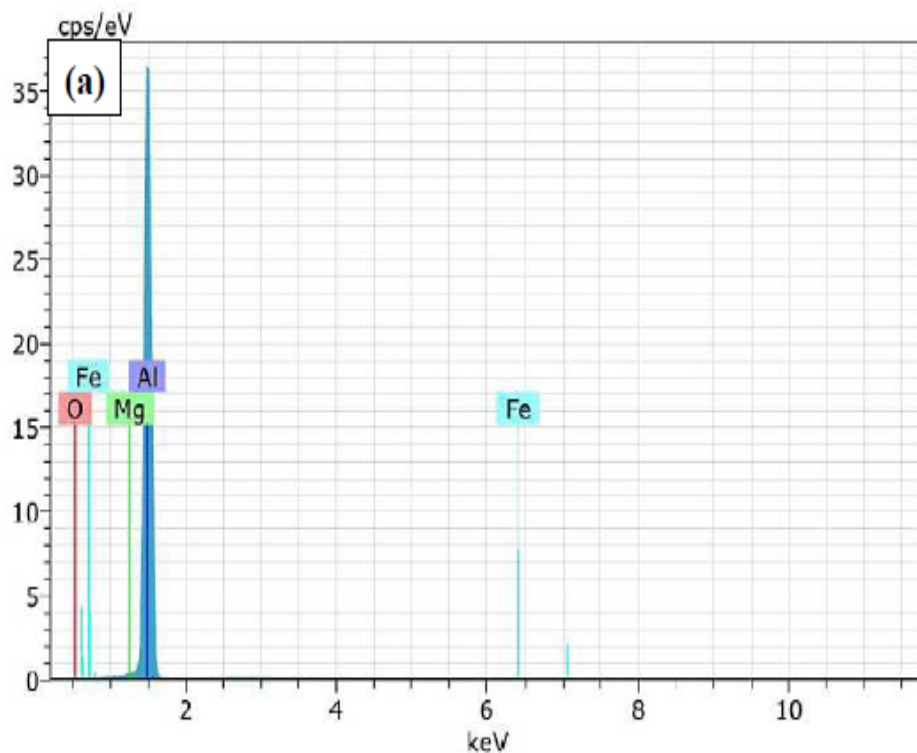
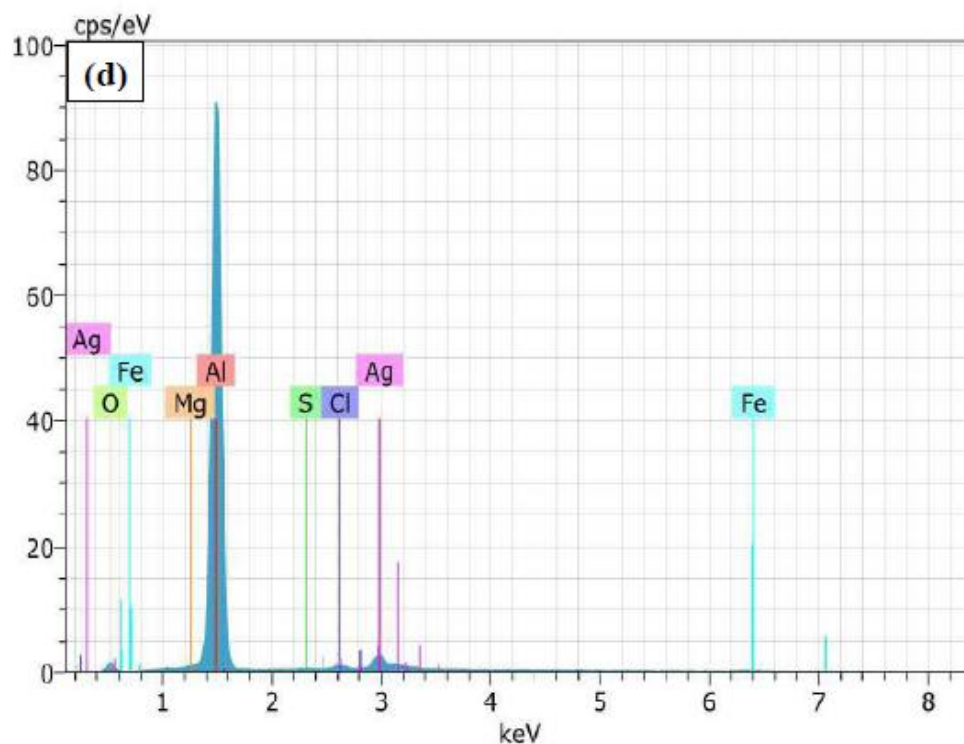
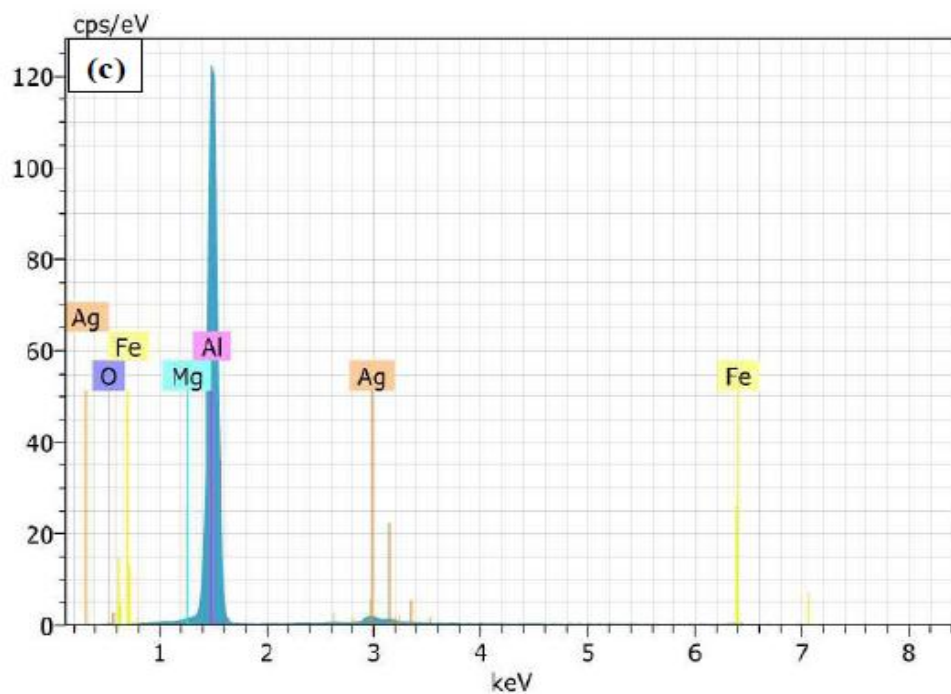


Figure 11- SEM morphologies of worn surface (a) Al6061 (b)Al6061-3% Ag (c) Al6061-6% Ag (d) Al6061-9% Ag (e) Al6061-12% Ag composite

### EDS ANALYSIS

EDS analysis confirms that the brighter area on Al6061 alloy sample worn surface beside aluminum element contains a considerable amount of oxygen and iron (Figure12a). In contrast, EDS analysis of the bright area on Al6061-Ag composite sample worn surface shows only the presence of Ag (Figure12 (b-e)). The presence of O and Fe in the darker layer implies the transfer of Fe from the steel pin to the worn surface while the oxygen element predicts the oxidation reaction. These results imply that transfer and mechanical mixing of materials have taken place between the two sliding surfaces, and a mechanically mixed tribo layer has been formed on the darker areas on the worn surface. This layer can act as an effective insulation layer between the pin and the disc, which prevents metal to metal contact. By comparing EDS analyses of the MML formed on the worn surfaces of 3%, 6%, 9% and 12% composite samples, it is revealed that 9% specimen has the highest Fe and 12% specimen has the highest O contents. Thus, these results show that higher reinforcement content in the Al6061-Ag composite promotes stronger material transfer from the counter face as well as oxidation reaction, while subsequently leads to quicker creation of more covering MML having elevated quantity of oxide compound composition on the worn surface, resulting to higher wear resistance.





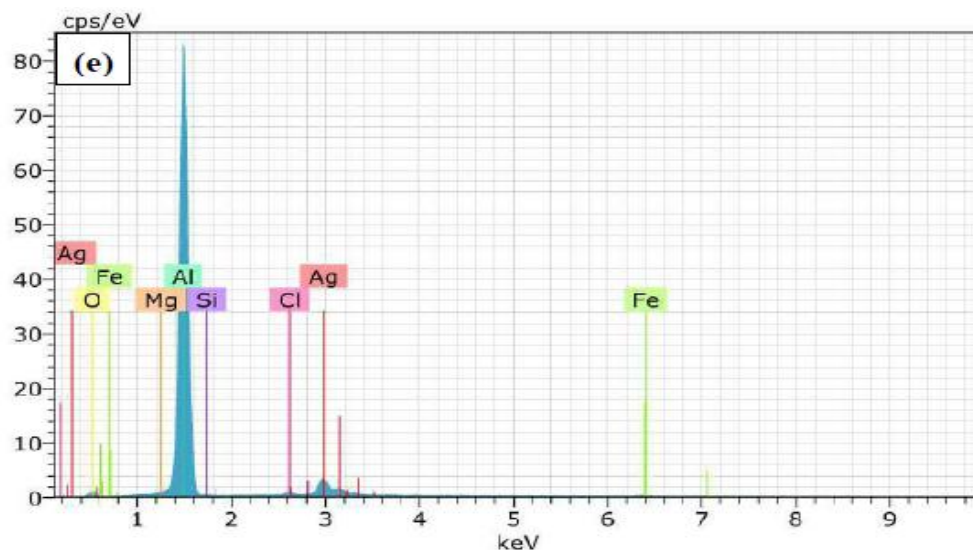


Figure 12:- EDS analysis of worn surface (a) Al6061 (b) Al6061-3% Ag (c) Al6061-6% Ag (d) Al6061-9% Ag (e) Al6061-12% Ag composite

## CONCLUSION

The mechanical, electrical, thermal and wear behavior studies and modeling work on Al6061- Ag composites are carried out effectively and the main conclusions arrived at from the experimental outcomes are detailed in this chapter.

- ❖ The silver powder is initially characterized by using XRD, SEM with EDS and particle size analyzer.
- ❖ Optical microscope studies of the cast composites show a homogeneous spreading of silver fortification in the Al6061 matrix. The studies revealed a uniform scattering of the reinforcement particles and good contact with the matrix material.
- ❖ A good increase in mechanical properties of the cast samples is shown with the addition of reinforcement particles. The hardness of the Ag added composites was critically enhanced while compared with the base material. The hardness of Al6061-9wt% Ag composites is above the base Al6061 alloy.
- ❖ Among the five different Al6061-Ag composites, electrical conductivity is found to be superior for Al6061-9 wt% Ag composite.
- ❖ It is concluded that reinforcing silver particle into the Al6061 alloy increases the crystallization and degradation temperature.
- ❖ Wear test was conducted on a pin-on disc wear tester in dry sliding situations of Al6061 alloy and Al6061-Ag composite. The addition of the weight percentage of Ag reinforcement content to Al6061, the specific wear rate decreases and also the frictional coefficient is controlled and reduced, when compared to the base Al6061 alloy material.
- ❖ The wear resistance tends to increase with the increasing wt.% of Ag, due to the formation of mechanical mixed layers. Consequently, it appears that a mechanical mixing/oxidation procedure is the mechanism of wear control in the case of Al6061-Ag composites.
- ❖ Moreover, the addition of the mechanical mixed tribo layers can also be visualized in SEM micrographs and EDS spectrum taken from the worn surface of the cast Al6061-Ag composite samples.
- ❖ Better frictional coefficient and wear resistance has been gained by the Al6061-Ag composites with the addition of 12% Ag particles.
- ❖ It is concluded from the statistical analysis that load and sliding distance are the major key factors which impact on the frictional coefficient and specific wear rate of the Al 6061-Ag composite.
- ❖ The results indicate that the load (51.68%) and sliding distance (19.37%) influences the specific wear rate of the composites, whereas sliding distance (30.11%) and load (22.55%) affect the frictional coefficient .

## **REFERENCES**

- Alidokht, SA, Abdollah-Zadeh, A, Soleymani, S, Assadi, H 2011, 'Microstructure and tribological performance of an aluminium alloy based hybrid composite produced by friction stir processing', *Materials and Design*, vol: 32, pp. 2727-2733.
2. Allwyn Kingsly Gladston, J, Mohamed Sheriff, N, Dinaharan, I & David Raja Selvam, J 2015, 'Production and characterization of rich husk ash particulate reinforced AA6061 aluminum alloy composites by compocasting', *Transactions of Nonferrous Metals Society of China*, vol.25, no. 683-691.
3. Amouri, K, Kazemi, S, Momeni, A & Kazazi, M 2016, 'Microstructure and mechanical properties of Al-nano/micro SiC composites produced by stir casting technique', *Materials Science and Engineering: A*, vol.674, pp. 569-578.
4. Anilkumar, HC, Hebbar, HS & Ravishankar, KS 2011, 'Mechanical properties of fly ash reinforced aluminium alloy (Al6061) composites', *International Journal of Mechanical and Materials Engineering*, vol. 6, pp. 41-45.
5. Balasivanaha Prabu, S 2006, 'Influence of stirring speed and stirring time on distribution of particles in cast metal matrix composite', *Journal of Materials Processing Technology*, vol. 171, pp. 268-273.
6. Baradeswaran, A & Elayaperumal, A 2014, 'Study on mechanical and wear properties of Al 7075/Al<sub>2</sub>O<sub>3</sub>/graphite hybrid composites', *Composites B*, vol. 56, pp. 464-471.
7. Baradeswaran, A & Elayaperumal, A 2013, 'Mechanical and tribological behaviour of graphite reinforced aluminium matrix composites', *Journal of the Balkan Tribological Association*, vol. 19, pp. 354-364.
8. Baradeswaran, A, Elayaperumal, A & Issac, RF 2013, 'A statistical analysis of optimization of wear behaviour of Al-Al<sub>2</sub>O<sub>3</sub> composites using Taguchi technique', *Procedia Engineering*, vol. 64, pp. 973-982.
9. Basavarajappa, S & Chandramohan, G 2006, 'Dry sliding wear behavior of metal matrix composites: A statistical approach', *Journal of Materials Engineering and Performance*, vol. 15, pp. 656-660.
10. Bharath, V, Nagaral, M, Auradi, V & Kori, SA 2014, 'Preparation of 6061Al-Al<sub>2</sub>O<sub>3</sub> MMC's by stir casting and evaluation of mechanical and wear properties', *Procedia Materials Science*, vol. 6, pp. 1658-1667.
11. Boopathi, MM, Arulshri, KP & Iyandurai, N 2013, 'Evaluation of mechanical properties of aluminium alloy 2024 reinforced with silicon carbide and fly ash hybrid metal matrix composites', *American Journal of Applied Sciences*, vol. 10, pp. 219-229.
12. Caton, MJ, Jones, JW, Boileav, JM & Allison, JE 1999, 'The effect of solidification rate on the growth of small fatigue cracks in a cast 319 type aluminum alloy', *Metallurgical and Materials Transactions A*, vol. 30, pp. 3055-3068.
13. Hashim, J, Looney, L & Hashmi, MSJ 1999, 'Metal matrix composites: Production by the stir casting method', *Journal of Materials Processing Technology*, vol. 92-93, pp. 1-7.
14. Iacob, G, Ghica, VG, Buzatu, M, Buzatu, T, Petrescu, MI 2015, 'Studies on wear rate and micro-hardness of the Al/Al<sub>2</sub>O<sub>3</sub>/Gr hybrid composites produced via powder metallurgy', *Composites Part B Engineering*, vol. 69, pp. 603-611.
15. Kalaiselvan, K, Murugan N, Sivaprameswaran 2011, 'Production and characterization of AA6061-B4C stir cast composite', *Materials and Design*, vol. 32, pp. 4004-4009.
16. Kaufman, JG 2002, 'Properties of aluminum alloys tensile creep and fatigue data at high and low temperatures', *ASM International*, pp. 7-17.

17. Kumar, A, Rao, C, Selvaraj, N & Bhagyathekar, M 2010, 'Studies on Al6061-SiC and Al7075-Al<sub>2</sub>O<sub>3</sub> metal matrix composites', Journal of Minerals and Materials Characterization and Engineering, vol. 9, pp. 43-55.
18. Li, WR, Xie, XB, Shi, QS, Zeng, HY, Ou-Yang, YS & Chen, YB 2010, 'Antibacterial activity and mechanism of silver nanoparticles on Escherichia coli', Applied Microbiology Biotechnology, vol. 85, pp. 1115-1122.
19. Mathur, S & Barnawal, A 2013, 'Effect of process parameter of stir casting on metal matrix composites', International Journal of Scientific Research, vol. 2, pp. 395-398.
20. Song M, chen K-H & Huang L-P 2006, 'Effects of Ag addition on mechanical properties and microstructures of Al-8Cu-0.5Mg alloy', Transactions of Nonferrous Metals Society of China, vol. 16, pp. 766-771.
21. Mishra, AK, Sheok and, R & Srivastava, RK 2012, 'Tribological behaviour of Al-6061/SiC metal matrix composite by Taguchi's techniques', International Journal of Scientific Research Publications, vol. 2, pp. 1-8.
22. Moses, JJ, Dinaharan, I & Sekhar, SJ 2014, 'Characterization of silicon carbide particulate reinforced AA6061 aluminum alloy composites produced via stir casting', Procedia Materials Science, vol. 5, pp. 106-112.
23. Paray, F, Kulunk, B & Gruzleski, JE 2000, 'Impact properties of Al-Si foundry alloys', International Journal of Casting Metals Research, vol. 13, pp. 17-37.
24. Suresha, S & Sridhara, BK 2011, 'Friction characteristics of aluminium silicon carbide graphite hybrid composites', Materials and Design, vol. 34, pp. 576-583.
25. Suresh, S & Moorthi, NSV 2013, 'Process development in stir casting and investigation on microstructures and wear behavior of TiB<sub>2</sub> on Al6061 MMC', Procedia Engineering, vol. 64, pp. 1183-1190.
26. Suresh, S, Shenbaga Vinayaga Moorthi, N, Vettivel, SC & Selvakumar, N 2014, 'Mechanical behavior and wear prediction of stir cast Al-TiB<sub>2</sub> composites using response surface methodology', Materials & Design, vol. 59, pp. 383-396.
27. Su, H, Gao, W, Feng, Z & Lu, Z 2012, 'Processing, microstructure and tensile properties of nano-sized Al<sub>2</sub>O<sub>3</sub> particle reinforced aluminum matrix composites', Materials and Design vol. 36, pp. 590-596.
28. Ravindran, P, Manisekar, K, Narayanasamy, R & Narayanasamy, P 2013b, 'Tribological behaviour of powder metallurgy- processed aluminium hybrid composites with the addition of graphite solid lubricant', Ceramic International, vol. 39, pp. 1169-1182.
29. Ritesh Raj, Dineshsingh, G & Thakur 2016, 'Qualitative and quantitative assessment of micro structure in Al-B4C metal matrix composite processed by modified stir casting technique', Archives of Civil and Mechanical Engineering, vol. 16, no. 4, pp. 949-960.
30. Rana RS, Rajesh Purohit & Das, S 2012, 'Reviews on the influences of alloying elements on the microstructure and mechanical properties of aluminum alloys and aluminum alloy composites', International Journal of Scientific and Research Publications, vol. 2, pp. 1-7.
31. Rao, VR, Ramanaiah, N & Sarcar, MMM 2015, 'Dry sliding wear behaviour of Al7075 reinforced with titanium carbide (TiC) particulate composites', Proceedings of International Conference on Advances in Materials, Manufacturing and Applications, pp. 39-44.